PHYSICAL REVIEW B **81**, 100407(R) (2010)

Influence of deposition field on the magnetic anisotropy in epitaxial $Co_{70}Fe_{30}$ films on GaAs(001)

A. T. Hindmarch,[1] D. A. Arena,[2] K. J. Dempsey,[1] M. Henini,[3] and C. H. Marrows[1]
[1]*School of Physics & Astronomy, University of Leeds, Leeds LS2 9JT, United Kingdom*
[2]*National Synchrotron Light Source, Brookhaven National Laboratory, Upton, New York 11973, USA*
[3]*School of Physics & Astronomy, Nottingham Nanotechnology and Nanoscience Centre, University of Nottingham, Nottingham NG7 2RD, United Kingdom*

(Received 27 January 2010; published 10 March 2010)

The effect of the application of a magnetic field during deposition of epitaxial $Co_{70}Fe_{30}$ onto GaAs(001) is shown; we find an initially counterintuitive result. For field applied along the interfacial uniaxial *hard* axis the relative effective uniaxial magnetic anisotropy is increased by a factor of two in comparison to both field along the uniaxial easy axis, or no field; usually, application of a deposition field results in a uniaxial easy axis parallel to this field direction. We show that the deposition field changes the maximal projection of the atomic orbital magnetic moments onto the easy axis, which corresponds to a deposition field induced shift in the Helmholtz free-energy landscape of the system.

DOI: 10.1103/PhysRevB.81.100407 PACS number(s): 75.30.Gw, 75.50.Bb, 75.70.−i

Proper understanding of the origins of giving the ability to manipulate magnetic anisotropies in ferromagnetic (FM) thin films is of vital importance for spintronics applications. The magnetization (***M***) direction in FM storage and processing elements must be both stable and controllable; commonly achieved by providing a mechanism by which a uniaxial magnetic anisotropy (UMA) may arise, confining ***M*** to preferentially lie parallel or antiparallel to a uniaxial easy axis (UEA).[1] UMA energy is the *difference* in the Helmholtz free energy for ***M*** parallel and perpendicular to the UEA.

A commonly employed method for inducing UMA is to apply a magnetic "forming" field during deposition of thin FM films. This has long been known to produce a *volume* "magnetization-induced" UMA,[2] with UEA oriented along the direction of the applied deposition field: similar effects may be observed due to annealing in a magnetic field.[3] ***M***-induced anisotropies are frequently and, most successfully, described in terms of the phenomenological Néel "pair ordering" model,[4] whereby the UMA arises due to a directional ordering of atom pairs in a polycrystalline or amorphous FM. Additionally, ***M***-induced UMA is suggested to arise due to a strain-magnetostriction mechanism, in situations where the lattice constant is constrained by the substrate;[5] magnetostriction is linked to the spin-orbit interaction in the FM film.

Another well-known example of UMA is that observed in FM films deposited onto the (001) surface of zinc-blende semiconductors (SCs), a prototypical system in FM/SC hybrid spintronics.[6–9] This uniaxial *interface* anisotropy, typically having UEA oriented along the in-plane [110] direction when combined with the comparably strong cubic magnetocrystalline anisotropy of a given epitaxial bcc-FM film, results in two-stage magnetization reversal for fields applied along $[1\bar{1}0]$, depicted schematically in the inset to Fig. 1(b): the straight arrow represents a coherent rotation of ***M***, while curved arrows represent abrupt changes in magnetization direction. The strength of the UMA determines the points at which ***M*** jumps between the uniaxial hard axis (UHA) and cubic easy axis (CEA). The mechanism by which interfacial UMA arises in these systems is still not at all well understood[6–8] but is thought to be related to the spin-orbit interaction in the underlying SC.[9,10]

In this Rapid Communication, we discuss the magnetic anisotropy in epitaxial sputter deposited bcc-$Co_{70}Fe_{30}$ films on GaAs(001), which have an in-plane magnetic field applied during film deposition. One may anticipate that such epitaxial films will exhibit a large UMA contribution due to, e.g., strain magnetostriction. However, magnetic fields are not commonly applied during molecular-beam epitaxy (MBE) deposition of such films, as the magnetic field precludes the use of surface electron diffraction methods to monitor epitaxial film growth. Only by combining magnetization- and interface-induced UMA contributions we

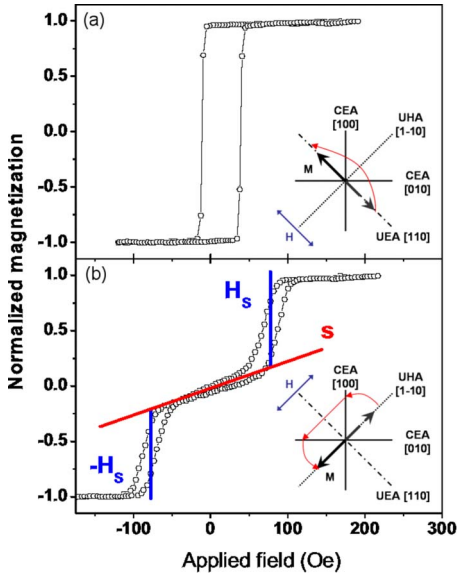

FIG. 1. (Color online) Room-temperature MOKE hysteresis loops for $Co_{70}Fe_{30}$[35 Å]/GaAs(001) deposited in zero applied field: the measurement field is applied along the two orthogonal in-plane {110} directions corresponding to the uniaxial (a) easy and (b) hard axes. The lower frame shows two-stage magnetization reversal, typical of thin bcc-FM films on GaAs⟨001⟩ surfaces. The zero-field reversible slope *s* (diagonal line) and shift field H_S (vertical lines) features are indicated. The insets show schematically how magnetization reversal occurs for magnetic field *H* applied along these two orthogonal directions.

are able to demonstrate the counterintuitive influence of the deposition field on the magnetic anisotropy of epitaxial $Co_{70}Fe_{30}$/GaAs(001).

The GaAs/AlGaAs heterostructure was grown by MBE onto a 2 in. diameter p^+-GaAs(001) wafer. The heterostructure consists of a p-$Al_{30}Ga_{70}As$/GaAs/n-$Al_{30}Ga_{70}As$ quantum-well LED with an i-GaAs[50 Å] interface layer. The structure was capped with arsenic in order to prevent atmospheric oxidation on removal from the MBE chamber. $Co_{70}Fe_{30}$[35 Å]/Ta[25 Å] films were deposited by dc magnetron sputtering, using a $Co_{70}Fe_{30}$ alloy sputter target in a separate vacuum chamber after thermally desorbing the As capping layer. Film deposition is described elsewhere and results in well ordered epitaxial CoFe films[11,12] and clean SC/FM interfaces.[9,12]

Magnetic measurements were made at room temperature by longitudinal magneto-optical Kerr effect (MOKE) using a HeNe laser with spot-diameter of ~0.5 mm. Soft x-ray magnetic circular dichroism (SXMCD) measurements were made at the U4B beamline at NSLS, Brookhaven. The beamline was operated with a circular polarization of ~90% and energy resolution of ~1.0 eV at the Co L_{III} edge, and data were collected in total-electron yield mode. Further details of the SXMCD measurement methods may be found in Refs. 9 and 13.

Here we discuss three particular $Co_{70}Fe_{30}$/GaAs(001) structures: two $Co_{70}Fe_{30}$ films were deposited with an in-plane magnetic field of $H_{Dep} \sim 175$ Oe, supplied by an array of permanent magnets inserted into the vacuum chamber close to the sample position. The field was applied parallel to one of the substrate {110} directions during film deposition: the two pieces were cut from a single wafer and one was rotated by 90° relative to the other; one sample had the deposition field applied along [110], while for the other it was applied along $[1\bar{1}0]$. The third sample—with nominally *zero* deposition field—was deposited onto a third piece cut from the same wafer, in a separate vacuum cycle, after removing the permanent magnet array. As all samples come from adjacent areas of a single 2 in. diameter GaAs wafer we assume that any substrate miscut is consistent between the samples studied.

Figure 1 shows MOKE hysteresis loops for $Co_{70}Fe_{30}$/GaAs deposited in zero magnetic field and measured with magnetic field applied along the GaAs [110] and $[1\bar{1}0]$. The multistage magnetization reversal along the UHA is indicative of the anticipated well-ordered bcc-FM on zinc-blende SC.

In general, following the method outlined in Refs. 14 and 15, we are able to extract the effective uniaxial anisotropy constant K_U^{eff} and first-order effective cubic anisotropy constant K_1^{eff} from the hysteresis loops measured along the UHA, assuming that the magnetization reversal around zero applied field takes place by a coherent rotation. We note that for $Co_{70}Fe_{30}$ the second order cubic anisotropy constant $K_2 \approx 0$ (Ref. 1) and that, due to the negligible (~0.3%) lattice mismatch with GaAs, magnetoelastic terms may be ignored in the absence of deposition field.[1,8,14] It is common also to neglect such magnetoelastic terms for the Fe/GaAs(001) system, despite the significantly larger ~1.4% lattice

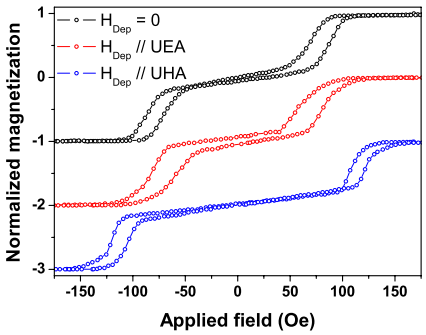

FIG. 2. (Color online) Comparison of room temperature MOKE hysteresis loops for $Co_{70}Fe_{30}$[35 Å]/GaAs(001) with the measurement field applied along the UHA, $[1\bar{1}0]$. During deposition of the structures the applied magnetic field was either zero (top), parallel to UEA (mid), or parallel to UHA (lower). Loops are offset for clarity. When the applied deposition field is parallel to UEA it does not significantly influence the magnetic anisotropy, cf. deposition in zero field.

mismatch.[15,16] The effective anisotropy constants are typically composed of volume and interface terms $K_a^{eff} = K_a^{vol} + K_a^{int}/t$, where $a = U$, 1, 2, etc., and t is the film thickness. The effective anisotropy constants may be calculated from the shift-field H_s and zero-field slope s indicated in Fig. 1. For thin MBE-grown bcc-FM/GaAs(001) one typically finds $K_U^{vol} \approx 0$ and $K_1^{vol} \gg K_1^{int}$; the UMA is purely interfacial in origin and the cubic magnetocrystalline anisotropy has a weak thickness dependence due to truncated crystal symmetry. Attempts have been made in the Néel model to qualitatively explain the thickness dependence of cubic magnetocrystalline anisotropy.[16]

For the film deposited in the absence of an applied deposition field we obtain values for the intrinsic cubic and uniaxial anisotropy constants for $Co_{70}Fe_{30}$[35 Å]/GaAs(001) of $K_1^{eff} = -2.8 \times 10^5$ erg/cc, $K_U^{eff} = 1.5 \times 10^5$ erg/cc, and thus $K_1^{eff}/K_U^{eff} = -1.9$, all in very good agreement with MBE-grown CoFe films of similar composition and thickness deposited onto GaAs(001).[14–16]

As we are able to safely draw comparison between our epitaxial sputtered $Co_{70}Fe_{30}$/GaAs(001) and similar MBE-grown material, we now move on to consider the films with magnetic field applied along one of the in-plane {110} directions during deposition. One could anticipate that the deposition field will induce a weak volume component to the UMA which may modify K_U^{eff} in some way: MOKE hysteresis loops measured along the UHA are shown in Fig. 2, for (mid trace) deposition field applied *parallel* to the interface induced UEA, i.e., the axis along which $\boldsymbol{M}$ would also lie in the absence of an applied magnetic field. The hysteresis loop for this film, measured with field applied along the UHA, appears similar to that for the film without deposition field. For this film we obtain $K_1^{eff} = -2.8 \times 10^5$ erg/cc, $K_U^{eff} = 1.4 \times 10^5$ erg/cc, and $K_1^{eff}/K_U^{eff} = -2.0$; very close to the values for the film deposited in zero field, consistent with $\boldsymbol{M}$-induced UMA.

The lower trace in Fig. 2 shows the corresponding hysteresis loop for the sample with deposition field applied parallel to the interface induced UHA *perpendicular* to the

TABLE I. Summary of the effective uniaxial and cubic magnetic anisotropy constants and SXMCD m_l/m_s component along the UEA for $Co_{70}Fe_{30}$[35 Å]/GaAs(001).

	$H_{dep}=0$	H_{dep}//UEA	H_{dep}//UHA
K_U^{eff} ($\times 10^5$ erg/cc)	1.5 ± 0.1	1.4 ± 0.1	2.1 ± 0.1
K_1^{eff} ($\times 10^5$ erg/cc)	-2.8 ± 0.1	-2.8 ± 0.1	-2.2 ± 0.1
K_1^{eff}/K_U^{eff}	-1.9 ± 0.1	-2.0 ± 0.1	-1.05 ± 0.1
m_l/m_s (Co)	0.21 ± 0.02	0.27 ± 0.02	0.14 ± 0.02
m_l/m_s (Fe)	0.11 ± 0.02	0.18 ± 0.02	0.10 ± 0.02

UEA. In this case we find $K_1^{eff}=-2.2\times10^5$ erg/cc, $K_U^{eff}=2.1\times10^5$ erg/cc, and $K_1^{eff}/K_U^{eff}=-1.05$. The effective anisotropy constants are summarized in Table I. We can estimate the strain-magnetostriction contribution to $K_U^{eff}\sim\frac{3}{2}Y\lambda^2\approx0.3\times10^5$ erg/cc,[5] where $Y\sim200$ GPa is the bulk Young's modulus and $\lambda\sim1\times10^{-4}$ the Joule magnetostriction:[1] the magnitude appears to be comparable to the measured difference in K_U for growth field along UHA. However, contrary to the data in Fig. 2, the strain-magnetostriction mechanism should *increase* the UMA for growth field along the interface-induced UEA, and *decrease* UMA for growth field applied along the interface-induced UHA.

Three points are noteworthy here: on changing the deposition field direction the UMA has effectively *doubled* relative to the cubic magnetocrystalline anisotropy; this has occurred not only through an increase in K_U^{eff} but also by a slight decrease in K_1^{eff}, and applying a deposition field along the UHA *increases* the UMA rather than decreasing it.

We can explain why applying a deposition field parallel to the UHA influences both the uniaxial *and* the cubic magnetocrystalline anisotropies by considering Néel's pair bonding model; here the interaction energy w between pairs of moments located on an undistorted cubic lattice,

$$w=d_2\left(\cos^2\phi-\frac{1}{3}\right)+q_4\left(\cos^4\phi-\frac{6}{7}\cos^2\phi+\frac{3}{35}\right)+\cdots,$$

are described by terms with isotropic (constant), uniaxial ($\cos^2\phi$), and cubic ($\cos^4\phi$) symmetry. ϕ is the angle between $\boldsymbol{M}$ and the pair-axis unit vector and d_2 (q_4) represent the pseudodipole (quadrupole) interaction energies: the total energy density and hence anisotropy constants result from summing over pairs of lattice sites.[4,16] Volume and interface anisotropy terms are separable within the Néel model as the anisotropy constants K_a^{vol} and K_a^{int} differ in the number of nearest-, next-nearest, etc. neighbors over which the w are summed for a "bulk" or "surface" lattice site.[16]

Within the Néel model it is clear that UMA and cubic anisotropy *should* be linked in some way, as both symmetries contribute to the pseudoquadrupole and higher-order terms. Thus the volume components of the uniaxial and cubic magnetocrystalline anisotropies may be coupled as may the interfacial components. It is perhaps not surprising that inducing a *volume* UMA component by applying a deposition field can also result in modification to the effective cubic magnetocrystalline anisotropy, as seen in Fig. 2. Beyond this the Néel model is no longer instructive: it is still unclear how applying a deposition field along UHA *increases* UMA.

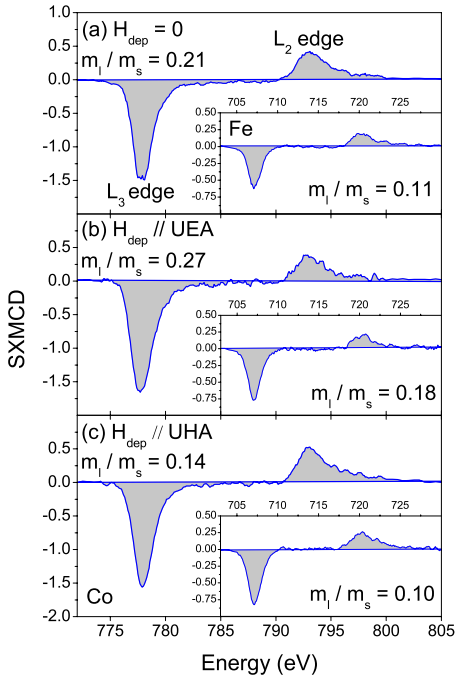

FIG. 3. (Color online) Room-temperature SXMCD spectra around the Co (main) and Fe (inset) L_{II} and L_{III} edges for $Co_{70}Fe_{30}$[35 Å]/GaAs(001) deposited with (a) zero magnetic field, (b) magnetic field applied along the UEA, and (c) magnetic field applied along the UHA. Measurement field is along UEA: the ratios of the m_l/m_s along the UEA, extracted from sum-rule analysis using the integrated SXMCD (shaded), are indicated.

A more correct picture of magnetic anisotropy is that it can be thought of as being related, via the spin-orbit interaction, to the anisotropy in the orbital magnetic moment associated with each lattice site. In Fe, Co, and their alloys, the 3d band is over half-filled; the spin-orbit coupling should restrict the maximal component of the orbital moment vector $\boldsymbol{m}_l$ to be parallel to the spin moment vector $\boldsymbol{m}_s$ (and hence $\boldsymbol{M}$) provided $\boldsymbol{M}$ is aligned along a high-symmetry direction.[17] This minimizes the leading (spin-orbit) term in the magnetic anisotropy energy, $\Delta E_{SO}\propto-\boldsymbol{m}_l\cdot\boldsymbol{m}_s$ (Ref. 18); in systems where UMA *dominates* then $\Delta E_{SO}^{UMA}\propto m_l^{UEA}-m_l^{UHA}$ (Ref. 19) and the component of $\boldsymbol{m}_l$ along the UEA (m_l^{UEA}, henceforth m_l) is often considered to be a measure of the degree of anisotropy in $\boldsymbol{m}_l$.[20] We note that in the case of $Co_{70}Fe_{30}$/GaAs(001), there are competing cubic and uniaxial anisotropies of comparable strength; one may imagine that the situation could be somewhat more complex.

Using the SXMCD technique it is possible to extract the orbital and spin components of atomic magnetic moments (per valence hole) with element specificity.[9,21] Figure 3 shows SXMCD spectra around the Co L_{II} and L_{III} edges for the three $Co_{70}Fe_{30}$ films on GaAs(001). SXMCD spectra around the Fe L_{II} and L_{III} edges are also shown in the insets. The applied magnetic field in our measurement geometry is limited to ~100 Oe to avoid Lorentz deflection artifacts in the sample drain current; we performed SXMCD measure-

ments in a ±23 Oe hold field after applying a saturating magnetic field, both parallel to the UEA as in Fig. 1(a). As our film thicknesses are comparable to the photoelectron escape depth, sum-rule analysis[21] of these data yields the *escape-depth weighted average* ratio of the components m_l/m_s along the UEA; we do not explicitly know the 3d hole density for $Co_{70}Fe_{30}$ so report the values of the ratio m_l/m_s in Table I.

$Co_{70}Fe_{30}$ deposited on GaAs(001) in zero field [Fig. 3(a)] has $m_l/m_s(\mathrm{Co})=0.21$ and $m_l/m_s(\mathrm{Fe})=0.11$; both of which are comparable to values for epitaxial CoFe.[20] We turn our attention to the $Co_{70}Fe_{30}$ films deposited onto GaAs(001) in the presence of an applied magnetic field: SXMCD spectra for these films are also shown in Fig. 3. In both films deposited in an applied field, the changes in the Fe L_{II} and L_{III} dichroism are similar to those for Co; were these changes related to interfacial bonding with GaAs, the dichroism from Co and Fe sites would not behave similarly.[9] We note that as the m_l/m_s are weighted average values they are essentially biased toward the *volume* rather than interfacial moments in this instance; one thus may obtain little information on the origin of the *interfacial* UMA from SXMCD on epitaxial CoFe/GaAs(001).

Figure 3(b) shows SXMCD for the film deposited with magnetic field applied parallel to the interfacial UEA. Here we find $m_l/m_s(\mathrm{Co})=0.27$ and $m_l/m_s(\mathrm{Fe})=0.18$; in both cases enhanced over the $Co_{70}Fe_{30}$ film deposited in zero field. In comparison to zero field deposition it appears that the m_l/m_s change via both an increase in the orbital moment and slight reduction in spin moment (larger net integrated dichroism and smaller integrated L_{II} dichroism, respectively[22]) from inspection of the integrated-SXMCD spectra. This *enhancement* in m_l means that the spin-orbit component of the free energy for $\boldsymbol{M}$ along UEA is larger (more negative) than that for zero deposition field. As the anisotropy constants K_{U} and K_1—and hence also ΔE_{SO} and the *in-plane* anisotropy in $\boldsymbol{m}_l$—do not change, the free energies for $\boldsymbol{M}$ along UEA, UHA, and cubic anisotropy axes must all be lowered equally; the *entire* Helmholtz free-energy *landscape* for in-plane reversal is shifted to lower energy by the application of a magnetic field along the interface-induced UEA during FM film deposition.

SXMCD for $Co_{70}Fe_{30}$/GaAs(001) with deposition field applied parallel to UHA is shown in Fig. 3(c). Here $m_l/m_s(\mathrm{Co})=0.14$ and $m_l/m_s(\mathrm{Fe})=0.10$; the ratio of orbital to spin moment is suppressed relative to zero field deposition for Co sites and also (much less so) for Fe. Applying a deposition field along UHA has the opposite effect to applying a deposition field along UEA: it decreases the component of $\boldsymbol{m}_l$ along UEA and hence *increases* the total free energy for $\boldsymbol{M}$ lying *along* UEA, relative to the other films. However, in contrast to the other films, for deposition field applied along UHA the large increase in UMA means that the in-plane anisotropy in $\boldsymbol{m}_l$ must also be modified. The raising of the free-energy landscape could result in a redistribution of electron states (e.g., via bonding charge transfer) between atomic levels on Co and Fe sites. We postulate that this could account for both the combination of increased K_{U} and slightly decreased K_1—which may be thought of as phenomenologically related to such "bonding" within the Néel model—and the smaller reduction in m_l/m_s(Fe) than in m_l/m_s(Co) when compared to deposition conditions where $\boldsymbol{M}$ lies along the interface-induced UEA during FM film growth.

In conclusion, we have demonstrated that the application of a magnetic field during epitaxial growth of bcc-CoFe on GaAs(001) can result in significant enhancement of the uniaxial magnetic anisotropy of the FM film; counterintuitively, the anisotropy is enhanced only when the field is applied along the interface-induced uniaxial hard axis. Applying the deposition field along the interfacial uniaxial easy (hard) axis produces an increase (decrease) in the component of the ratio of the atomic species resolved orbital and spin magnetic moments, m_l/m_s, directed along the uniaxial easy axis of magnetization. In conjunction with cubic and uniaxial anisotropy constants extracted from magnetic hysteresis measurements, we discuss how this corresponds to a net lowering (raising and distortion) of the overall Helmholtz free-energy landscape.

The authors acknowledge financial support from EPSRC and from the EU via Project No. NMP2-CT-2003-505587 "SFINx." We are grateful to Brookhaven National Laboratory for the provision of NSLS beamtime and thank D. Taylor for assistance with MBE wafer preparation.

[1] R. M. Bozorth, *Ferromagnetism* (Van Nostrand, New York, 1951).
[2] M. S. Blois, Jr., J. Appl. Phys. **26**, 975 (1955).
[3] R. M. Bozorth, Rev. Mod. Phys. **25**, 42 (1953).
[4] L. Néel, J. Phys. Radium **15**, 225 (1954).
[5] F. G. West, J. Appl. Phys. **35**, 1827 (1964).
[6] J. J. Krebs *et al.*, J. Appl. Phys. **61**, 2596 (1987).
[7] G. A. Prinz, Science **250**, 1092 (1990).
[8] O. Thomas *et al.*, Phys. Rev. Lett. **90**, 017205 (2003).
[9] A. T. Hindmarch *et al.*, Phys. Rev. Lett. **100**, 117201 (2008).
[10] E. Sjöstedt *et al.*, Phys. Rev. Lett. **89**, 267203 (2002).
[11] A. T. Hindmarch *et al.*, J. Appl. Phys. **101**, 09D106 (2007).
[12] A. T. Hindmarch *et al.*, J. Appl. Phys. **105**, 073907 (2009).
[13] A. T. Hindmarch *et al.*, Appl. Phys. Lett. **93**, 172511 (2008).
[14] F. Bianco *et al.*, J. Appl. Phys. **104**, 083901 (2008).
[15] M. Dumm *et al.*, J. Appl. Phys. **87**, 5457 (2000) where incorrect expressions for the anisotropy constants are given.
[16] M. Dumm *et al.*, J. Appl. Phys. **91**, 8763 (2002) and references therein.
[17] H. A. Dürr *et al.*, Science **277**, 213 (1997).
[18] P. Bruno, Phys. Rev. B **39**, 865 (1989).
[19] D. Weller *et al.*, Phys. Rev. Lett. **75**, 3752 (1995).
[20] F. Yildiz *et al.*, Phys. Rev. Lett. **100**, 037205 (2008).
[21] C. T. Chen *et al.*, Phys. Rev. Lett. **75**, 152 (1995).
[22] J. Stöhr, J. Magn. Magn. Mater. **200**, 470 (1999).